[CANCER RESEARCH 60, 230–234, January 15, 2000]

Advances in Brief

Vascular Protection by Chloroquine during Brain Tumor Therapy with Tf-CRM107

Naoshi Hagihara, Stuart Walbridge, Alan W. Olson, Edward H. Oldfield, and Richard J. Youle[1]

Biochemistry and Clinical Sections, Surgical Neurology Branch, National Institute of Neurological Disorders and Stroke [N. H., S. W., E. H. O., R. J. Y.], and in Vivo NMR Research Center of National Institute of Neurological Disorders and Stroke [A. W. O.], National Institutes of Health, Bethesda, Maryland 20892

Abstract

Tf-CRM107 is a conjugate of transferrin and a point mutant of diphtheria toxin that selectively kills cells expressing high levels of the transferrin receptor. Tf-CRM107 has been infused intratumorally into patients with malignant brain tumors. Although approximately half of the patients exhibit tumor responses, patients receiving higher doses of Tf-CRM107 may develop magnetic resonance image (MRI) evidence of toxicity indicative of small vessel thrombosis or petechial hemorrhage. Consistent with these clinical results we found that intracerebral injection of Tf-CRM107 into rats at total doses ≥0.025 μg causes brain damage detectable by MRI and histology. To widen the therapeutic window of Tf-CRM107, we explored ways to prevent this damage to the vasculature. We reasoned that the vasculature may be protected to a greater extent than tumor from Tf-CRM107 infused into brain parenchyma by i.v. injection of reagents with low blood-brain barrier permeability that block the toxicity of Tf-CRM107. Chloroquine, a well-characterized antimalarial drug, blocks the toxicity of diphtheria toxin and Tf-CRM107. Systemic administration of chloroquine blocked the toxicity of Tf-CRM107 infused intracerebrally in rats and changed the maximum tolerated dose of Tf-CRM107 from 0.2 to 0.3 μg. Moreover, chloroquine treatment completely blocked the brain damage detected by MRI caused by intracerebral infusion of 0.05 μg of Tf-CRM107. In nude mice bearing s.c. U251 gliomas, chloroquine treatment had little effect on the antitumor efficacy of Tf-CRM107. Thus, chloroquine treatment may be useful to reduce the toxicity of Tf-CRM107 for normal brain without inhibiting antitumor efficacy and increase the therapeutic window of Tf-CRM107 for brain tumor therapy.

Introduction

The prognosis of patients with malignant brain tumors is poor despite standard therapy (surgery, radiation, and chemotherapy). Tf-CRM107 (1), a conjugate of Tf[2] and a mutant DT lacking receptor-binding function (2), can target and kill cells expressing Tf-R, such as tumor cells. The potential of Tf-CRM107 for brain tumor therapy has been explored *in vitro* (1), in animal models (3), and in patients with malignant gliomas (4). When delivered by high-flow (4–10 μl/min) interstitial microinfusion CED (5), intratumoral infusion of Tf-CRM107 in patients with malignant brain tumors produces tumor responses (4). When CED is used, Tf-CRM107 (140 kDa) is distributed preferentially into the interstitial space of the tumor and the surrounding brain infiltrated by tumor and circumvents the BBB. However, in the brain, capillary endothelial cells express low levels of Tf-R (6), and at high doses Tf-CRM107 can cause neurological deficits consistent with endothelial damage. MRI in these patients has revealed changes in the brain consistent with microvascular occlusion and/or petechial hemorrhage (4).

Our goal was to selectively protect CNS capillaries from Tf-CRM107 toxicity without protecting brain tumor cells. We sought a drug with low BBB permeability that could be delivered i.v. to protect the vasculature. Lysosomotrophic amines, such as chloroquine, are used clinically to treat malaria and certain collagen diseases. These drugs accumulate in lysosomes and increase and neutralize vesicular pH (7). DT enters the cell to inhibit protein synthesis, using the low pH of endosomes and lysosomes to trigger transport into the cytosol (8–11). Thus, chloroquine blocks the cytotoxicity of DT (12) and likely Tf-CRM107.

We investigated the potential of chloroquine to improve the utility of immunotoxins for brain tumor therapy by selectively suppressing toxicity to the vasculature without altering the antitumor efficacy.

Materials and Methods

Cell Lines and Animals. The U251MG human glioblastoma cell line and 9L rat gliosarcoma cell line were purchased from American Type Culture Collection. Both cell lines were grown in DMEM media supplemented with 10% FCS and maintained at 37°C in a 5% CO_2 environment. Animal experiments were performed with male Fisher 344 rats (Taconic), 20–25 weeks of age, with a body weight ranging from 250 to 300 g and NIH nu/nu female mice 4–6 weeks of age, which were cared for in accordance with NIH guidelines.

DT, Tf-CRM107, and Chloroquine. DT was purchased from List Biologicals (Campbell, CA). Preparation of the DT mutant CRM107 and its conjugation to human Tf were performed as described previously (1). The toxin and Tf were linked by a thioether bond. Chloroquine diphosphate salt (515.9 Da) was purchased from Sigma (St. Louis, MO). Toxins and chloroquine were dissolved in PBS for *in vitro* experiments and in 0.9% physiological saline for *in vivo* experiments.

Tf-R Expression. The mouse monoclonal anti-Tf-R antibody was purchased from ZYMED Laboratories (San Francisco, CA). This antibody (H68.4) is specific to residues 3–28 of the human Tf-R N-terminal tail and cross-reacts with rat Tf-R. The normal cerebrum, cerebellum, pons, medulla, and cervical segment of the spinal cord were removed from rats, and tumors were removed from rats bearing 9L brain tumors 14 days after tumor inoculation and frozen immediately in precooled isopentane with dry ice. The frozen tissues were homogenized with 1% Triton X-100 in PBS and centrifuged at 800 × *g*, and the supernatant was saved. The protein concentration of each tissue sample was determined by the BCA protein assay kit (Pierce, Rockford, IL). Equal quantities of protein were separated on 4–12% Tris-Glycine Gel (Novel Experimental Technology, San Diego, CA) with an equal volume of Tris-Glycine SDS sample buffer 2X (NOVEX). The proteins separated by PAGE were electroblotted onto Immobilon PVDF membranes (Millipore, MA) using TRNSBLOT (Bio-Rad Laboratories, Hercules, CA). After blocking with 0.05% Tween 20 (Sigma) in PBS (pH 7.4) containing 5% FCS, the membranes were incubated with the primary antibodies for 1 h at room temperature. The membranes were then washed and incubated with horseradish peroxidase-conjugated sheep antimouse IgG antibody (Amersham Pharmacis Biotech, Inc., Piscataway, NJ). After thorough washing, the immunoreactive proteins were visualized by the ECL system according to the manufacturer's directions (Amersham).

Received 4/5/99; accepted 9/3/99.

The costs of publication of this article were defrayed in part by the payment of page charges. This article must therefore be hereby marked *advertisement* in accordance with 18 U.S.C. Section 1734 solely to indicate this fact.

[1] To whom requests for reprints should be addressed, at Biochemistry Section, Building 10, Room 5D-37, MSC 1414, 10 Center Drive, Bethesda, MD 20892-1414. Phone: (301) 496-6628; Fax: (301) 402-0380; E-mail: youle@helix.nih.gov.

[2] The abbreviations used are: Tf, transferrin;, DT, diphtheria toxin; Tf-R, transferrin receptor; CED, convection-enhanced delivery; BBB, blood-brain barrier; MRI, magnetic resonance image; CNS, central nervous system; MTD, maximum tolerated dose.

***In Vitro* Cytotoxicity Assay.** The toxicity of Tf-CRM107 to U251MG cells after chloroquine treatment was studied using [^{14}C]leucine incorporation as a measure of protein synthesis, as reported previously (1). Briefly, after U251MG cells were incubated with leucine-free RPMI 1640 for 6 h, chloroquine was added and incubated for 1 h. Several doses of Tf-CRM107 (7×10^{-15} to 7×10^{-8} M) were then added; 12 h later, 0.1 μCi of [^{14}C]leucine was added, incubation was continued for 1 h, and then the cells were harvested. All cytotoxicity assays were performed three times. The results were expressed as a percentage of [^{14}C]leucine incorporation in mock-treated control cultures and were expressed as means ± SE.

MTD Assessment. After anesthesia (i.p. injection of 80 mg/kg ketamine and 12 mg/kg xylazine), rats were placed in a stereotactic frame. A midline sagittal incision was made, and a dental drill was used to place a burr hole 3 mm lateral and 1 mm anterior to the bregma. Toxins were infused for MTD determination in a volume of 5 μl intracerebrally into rats at 1 μl/min, using a 10-μl Hamilton syringe. DT was given to achieve total doses of 0.025–0.2 μg, and Tf-CRM107 was given to achieve total doses of 0.1–0.5 μg. The rats received i.p. injections of either chloroquine (45 mg/kg; $n = 41$) or vehicle (0.9% physiological saline; $n = 39$) 5 min before intracerebral injection and once each day for 5 consecutive days. We observed all rats for at least 14 days. If animals showed signs of distress (lethargy, neurological deficit, or inability to obtain food and water), they were euthanized and decapitated, and the brains were removed immediately for histology. We considered the maximum dose of toxin injected intracerebrally that did not cause distress to be the MTD.

MRI. MRI was performed on rats under anesthesia (i.p. injection of 80 mg/kg ketamine and 12 mg/kg xylazine) to detect brain damage.

For toxicity measurement under conditions of infusion identical to MTD measurements, MRI was performed 3 days after injection with 0.4 μg of Tf-CRM107 (1 μl/min). The protocol used on these images was spin-eco multislice done on a GE Omega 2 Tesla horizontal bore instrument with 4 gauss/cm shielded gradients. The T1-weighted image was taken with a TE/TR of 20/500 ms with a total scan time of 8.5 min. The T2-weighted images were taken with a TE/TR of 80/1500 ms with a total scan time of 51 min. Each of these slices had an in-plane digital resolution of 390 μm and 2-mm slice thickness.

To detect complete blocking of the toxicity of Tf-CRM107 by chloroquine in normal brain and to best model the infusion method used in clinical trials (CED), 0.05 μg of Tf-CRM107 in 5 μl were infused at 0.1 μl/min with a pressure gradient maintained using a syringe pump (Harvard Apparatus, S. Natick, MA), and the MRI was performed 14 days after infusion. The protocol used on these images was spin-echo multislice done on a Varian Inova 4.7 Tesla horizontal bore instrument with 15 gauss/cm shielded gradients. These T2-weighted images were taken with a TE/TR of 80/2000 ms; slice thickness was 1 mm with 1.5 mm between slice centers. Each of these slices had an in-plane digital resolution of 390 μm.

Tumor Model. Solid U251MG human glioma tumors were grown by injecting 10^7 cultured U251MG cells s.c. into the flanks of nude mice. Palpable tumors were detected after 4–5 weeks and reached 0.4–0.6 cm in diameter. Tumor size was evaluated by measuring two perpendicular diameters with Vernier calipers and using the formula $1/2LW^2$, where L is the longest diameter and W is the diameter perpendicular to L. Groups of five nude mice with established U251MG flank tumors were randomly assigned to receive intratumoral injections with 100 μl of either PBS or Tf-CRM107 (100 μg/ml; total dose, 10 μg) with or without chloroquine treatment. The mice received i.p. injections of either chloroquine (45 mg/kg; $n = 5$) or vehicle (0.9% physiological saline; $n = 5$) 5 min before intratumoral injection of Tf-CRM107 and once a day for 4 consecutive days at the same dose. Tumor volume, assessed for 10 days, was represented as a percentage of initial volume and expressed as a mean ± SE.

Results and Discussion

We compared the Tf-R levels in different regions of normal rat brain with the Tf-R level in 9L brain tumors. The Tf-R was detected as a homodimer (180 kDa) on Western blots. Normal brain (cerebrum, cerebellum, pons, medulla, and cervical segment of the spinal cord) expressed Tf-R with some variation in magnitude among different regions (Fig. 1*A*, *Lanes 1–5*). The pons expressed particularly low levels of Tf-R, possibly reflecting the lower capillary density in white matter than gray matter. 9L brain tumors 14 days after inoculation into rat brains were also examined. The degree of expression of Tf-R in 9L tumors was higher than that of the normal CNS (Fig. 1*A*, *Lane 6*).

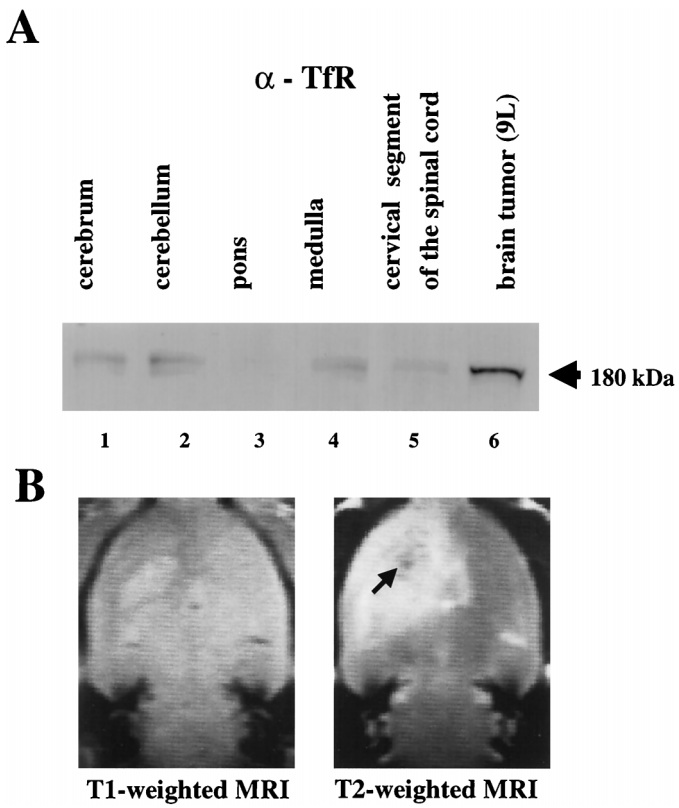

Fig. 1. *A*, Western blot analysis of Tf-R in Fisher 344 rats. Thirty μg of tissue extract were run on a 4–12% SDS-PAGE and stained with an anti-Tf-R antibody (ZYMED). The tissue samples were from normal rat (*Lanes 1–5*), and rats bearing 9L brain tumors 14 days after tumor inoculation (*Lane 6*). 9L brain tumor expresses more Tf-R compared with the CNS. *B*, T1-weighted MRI (*left*) and T2-weighted MRI (*right*) scans of rat brain 3 days after intracerebral infusion with 0.4 μg of Tf-CRM107. The large occupational area represented hemorrhage and involved edema. The central component [isointensity on the T1-weighted MRI and low intensity (indicated by the *arrow*) on the T2-weighted MRI] represented intact RBCs with deoxyhemoglobin after hemorrhage. The outer component (low intensity on the T1-weighted MRI and high intensity on the T2-weighted MRI) represented edema.

When 5 μl of Tf-CRM107 were infused into normal rat brain at 1 μl/min, total doses of 0.025 μg or more caused brain damage such as necrosis and encephalomalacia detected by histology by day 14 after infusion. These results were consistent with our previous reports (3).

We examined Tf-CRM107 toxicity to rat brain by MRI. MRI of rat brains 3 days after intracerebral injection with 0.4 μg of Tf-CRM107 revealed a mass lesion with two components of different signal intensities in the right frontal lobe. The central component was isointense on the T1-weighted MRI and low intensity on the T2-weighted MRI (Fig. 1*B*, *arrow*). These MRI patterns are consistent with intact RBCs containing deoxyhemoglobin after hemorrhage. The outer component was low intensity on the T1-weighted MRI and high intensity on the T2-weighted MRI (Fig. 1*B*), indicating edema with the large occupational area representing hemorrhage and involved edema. Histology of the lesion showed hemorrhage with necrosis, tissue loss, and invasion by macrophages (data not shown). These changes in the brain detected by MRI and histopathology indicate that Tf-CRM107 causes vascular damage. Tf-CRM107 at high doses may bind to Tf-Rs on capillary endothelial cells and cause thrombosis and then hemorrhagic infarction, or it may directly cause hemorrhage as a result of endothelial injury.

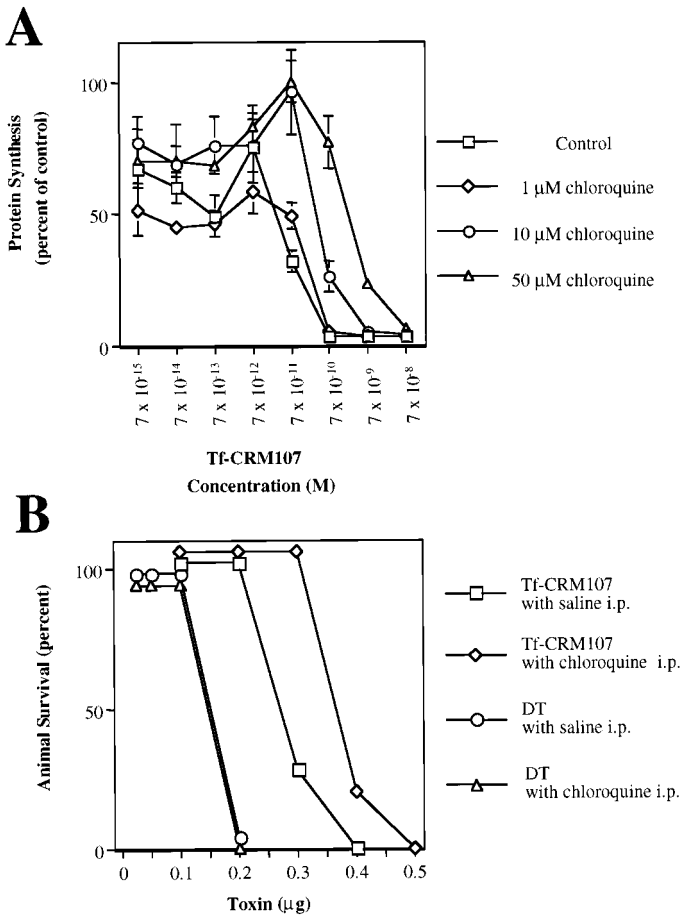

Fig. 2. *A*, toxicity of Tf-CRM107 to U251MG human glioma cells after 12-h exposure with and without chloroquine (1, 10, and 50 μM). Chloroquine was added to cells 1 h before Tf-CRM107. Tf-CRM107 without chloroquine (□) is the control. *B*, survival rate after intracerebral injection of toxins into rats. Rats received injections in the right frontal lobe with the indicated dose of DT and Tf-CRM107. Neurological symptoms and survival of animals were monitored. The percentage of survival of animals is plotted (three to seven animals per group).

Chloroquine is known to block the toxicity of DT *in vitro* (12). We found chloroquine *in vitro* blocked the toxicity of Tf-CRM107 10–100-fold, and at a concentration of Tf-CRM107 of 7×10^{-11} M, cells were completely protected by 10 μM chloroquine (Fig. 2*A*).

Rats receiving 0.4 μg of Tf-CRM107 exhibited clinical signs of toxicity. We postulated that systemic delivery of chloroquine may protect the CNS vasculature from Tf-CRM107 and decrease CNS toxicity *in vivo*. We examined the MTD of Tf-CRM107 with and without chloroquine administration. After intracerebral injection with 0.2 μg of Tf-CRM107, no remarkable symptoms were observed in five of five rats. However, five (71%) of the seven rats that received 0.3 μg of Tf-CRM107 showed signs of distress around day 6 after injection. Five of five rats that received 0.4 μg of Tf-CRM107 died around day 4. However, if rats received chloroquine (45 mg/kg) following injection with 0.3 μg of Tf-CRM107, zero of five animals showed signs of distress. Although 0.4 μg of Tf-CRM107 with chloroquine caused signs of distress in four (80%) of five animals, chloroquine increased the survival rate and changed the MTD of Tf-CRM107 from 0.2 μg to 0.3 μg (Fig. 2*B*). Thus, systemic chloroquine protects animals from intracerebral toxicity due to Tf-CRM107.

Intracerebral infusion with 0.05 μg of Tf-CRM107 caused histological brain damage (*i.e.*, necrosis) in the right frontal lobe by day 14. Toxicity at this dose was detected as a high-intensity lesion on T2-weighted MRI (Fig. 3, *left*). Systemic chloroquine administration (45 mg/kg) completely blocked the brain damage caused by 0.05 μg of Tf-CRM107 at day 14 ($n = 3$; Fig. 3, *right*).

Systemic chloroquine could protect the brain vasculature from intracerebrally infused Tf-CRM107. If chloroquine could decrease the toxicity of Tf-CRM107 without decreasing antitumor efficacy, an improved therapy for brain tumors may be possible. The BBB may be expected to limit the amount of chloroquine that can pass into the cerebral fluid, bathing brain tumor cells, and may prevent enough chloroquine from entering the brain to block the antitumor activity of Tf-CRM107. The brains of rats and mice are too small to accurately model brain tumor infusions; therefore, we used a surrogate measure of chloroquine entry into the brain. To assess whether enough chloroquine crosses the BBB to inhibit antitumor activity of Tf-CRM107, we used native DT that has a similar sensitivity to chloroquine (1, 12). In contrast to Tf-CRM107, which targets endothelial cells in the CNS, DT is selectively toxic to neurons in the rat brain (13) and thus targets a cell type on the CNS side of the BBB as brain tumor cells are. We checked the effect of systemic chloroquine on the survival rate of rats injected intracerebrally with DT. Although none of four rats that received 0.1 μg of DT showed signs of distress, all four rats that received 0.2 μg of DT showed signs of distress around day 5. When chloroquine was injected i.p. at 45 mg/kg in addition to 0.2 μg of intracerebral DT, all four animals showed signs of distress around day 5 (Fig. 2*B*). Thus, i.p. injection of chloroquine does not block toxicity of intracerebral DT. Although i.p. injection of chloroquine appears to reach and protect the brain vasculature from Tf-CRM107, it does not protect the CNS neurons from DT.

Contrast-enhancing brain tumors may have a partially defective BBB, and this may allow enough chloroquine into the brain tumor to block Tf-CRM107 efficacy. We tested this hypothesis, using a "worst-case scenario" of leaky tumor vasculature in the periphery. We injected Tf-CRM107 into U251 tumors grown in the flanks of nude mice with and without i.p. injection of chloroquine. Intratumoral injection of Tf-CRM107 significantly inhibited tumor growth compared with PBS ($P < 0.01$), and i.p. injection of chloroquine at 45 mg/kg caused little or no blocking of the efficacy of Tf-CRM107 against the s.c. tumor (Fig. 4).

Tf-CRM107 infused intratumorally using high-flow interstitial microinfusion into patients with recurrent malignant brain tumors caused

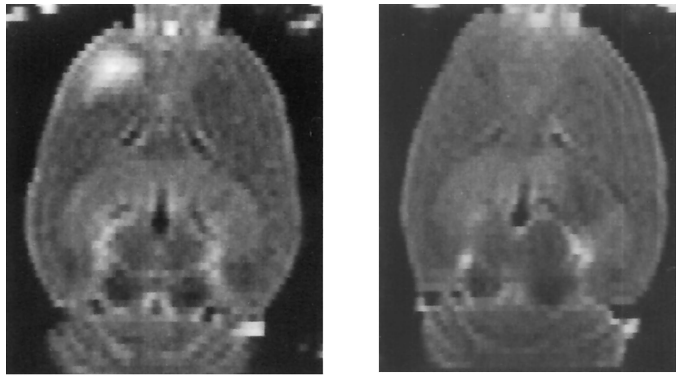

Fig. 3. T2-weighted MRI scan of a rat that received an intracerebral infusion with 0.05 μg of Tf-CRM107 (10 μg/ml) with 5 days i.p. injection of chloroquine (45 mg/kg; *right*) compared with a rat that received 0.9% physiological saline instead of chloroquine (*left*). Tf-CRM107 was microinfused at 0.1 μl/min using a syringe pump.

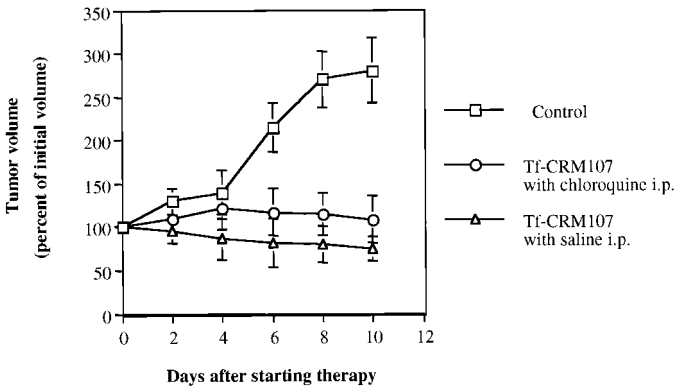

Fig. 4. Changes in U251MG s.c. tumor volume following intratumoral infusion of Tf-CRM107. Groups of five nude mice with flank tumors were randomly assigned to be injected intratumorally with 100 μl of PBS or 100 μl of Tf-CRM107 (total dose, 10 μg) with or without i.p. chloroquine treatment. Tumor volume is represented as the percentage of initial volume, assessed for 10 days and expressed as mean; *bars*, SE.

at least a 50% reduction in tumor volume in 8 of 15 patients (4). To improve on this outcome, we have considered ways to increase the dose of Tf-CRM107 safely to more effectively eradicate tumor cells. In that clinical study peritumoral, focal brain injury occurred in all patients who received 40 μg of Tf-CRM107 at 1 μg/ml. Histological analysis of biopsies revealed thrombosed cortical venules and/or capillaries. Thus, dose-limiting toxicity associated with intratumoral Tf-CRM107 infusion in humans is consistent with brain capillary endothelial damage. Tf-Rs are expressed on endothelial cells in normal brain (6). Although most Tf-Rs appear on the capillary lumen (6), they may cycle through the cell to the abluminal side where they may bind intracerebral Tf-CRM107. High doses of Tf-CRM107 may cause hemorrhagic infarction following diffuse vessel thrombosis or cause hemorrhage directly after binding to Tf-Rs on capillary endothelial cells. Intracerebral infusion of Tf-CRM107 into rat brains at doses $\geq$0.025 μg caused CNS damage detected by both histology and MRI. We detected MRI damage at 40 μg (roughly 0.8 μg/kg) of Tf-CRM107 in humans and at 0.025 μg (roughly 0.1 μg/kg) in rats. This discrepancy in MTD between rats and humans may in fact be due to differences in the infusion rate or infusion volume relative to the size of the brain. Because it may be implausible to continuously infuse rats over 5 days to precisely model infusions in humans, we have not been able to compare MTD directly between rats and humans by the same delivery technique.

We sought to overcome the dose-limiting toxicity of Tf-CRM107. To protect normal capillaries from Tf-CRM107, we identified a drug that would block Tf-CRM107. DT has a series of hydrophobic domains (14, 15) that insert into membranes when exposed to the low pH present in endosomes and lysosomes (8–11). Chloroquine blocks the toxicity of DT by increasing and neutralizing endosomal pH (7, 12) and blocks the toxicity of Tf-CRM107. Chloroquine also can increase the survival of rats after intracerebral Tf-CRM107 infusion and prevents the MRI changes associated with toxicity. The high intensity signal on T2-weighted MRI after infusion of Tf-CRM107 may reflect the histological damage due to thrombosed capillaries or petechial hemorrhage. Generally speaking, T2-weighted MRI is very sensitive for detection of this type of brain damage. Chloroquine treatment protected animals from this damage caused by Tf-CRM107.

We considered the extent to which chloroquine crosses the BBB. The most important factors determining drug delivery from blood into CNS are lipid solubility, molecular mass, and charge (16). The normal BBB inhibits the passage of water-soluble drugs with a molecular mass greater than 180 Da. Chloroquine (516 Da) is freely soluble in water and insoluble in alcohol, benzene, chloroform, or ether. Our experiments revealed that chloroquine did not change the MTD of intracerebrally injected DT and did not reduce the histological brain damage in rats that received DT (data not shown). On the other hand, chloroquine did block the toxicity of intracerebrally injected Tf-CRM107. The different sensitivities of intracerebral DT and Tf-CRM107 to systemic chloroquine supports the model that Tf-CRM107 is specifically targeting capillary endothelial cells. Chloroquine does not cross the BBB to a degree sufficient to block DT and thus should not block the antitumor efficacy of Tf-CRM107 injected intracerebrally.

We directly investigated whether chloroquine inhibited the antitumor efficacy of Tf-CRM107. The BBB is intact at the proliferating edges of malignant brain tumors and in regions of infiltrated brain but is more leaky in the center (17). In practice, clinical studies with computed tomography reveal that BBB permeability is variable in brain tumors (18). We found here that chloroquine treatment causes little or no blocking of the efficacy of intratumoral Tf-CRM107 even in s.c. tumors entirely lacking the BBB. The BBB should even further minimize chloroquine access to brain tumors. It appears that chloroquine may block the toxicity to the vasculature with little effect on the antitumor efficacy of Tf-CRM107 in brain.

Although some side effects are known, chloroquine has generally been considered safe and may be taken p.o. Eleven healthy volunteers given 300 mg of chloroquine as a single dose i.v. infusion complained only of subjective side effects, such as difficulties with swallowing and accommodation, diplopia, and fatigue during i.v. infusion; no effects were seen on the electrocardiogram, mean arterial blood pressure, or pulse rate (19). Patients unable to take oral doses might be given chloroquine by slow i.v. infusion or by s.c. or i.m. injection (20).

Computed tomography and MRI studies using i.v. contrast enhancement define the location of brain tumors because contrast media leaks from regions lacking an intact BBB. Although tumor resection is performed as precisely as possible according to scans of the enhancing lesion, the proliferating edge of tumor does not contrast enhance because the BBB remains intact and tumor cells are known to invade centimeters beyond the enhancing lesion (21–23). After surgical resection, this residual tumor in areas with an intact BBB is the major factor underlying the failure of current treatments of these patients. Tf-CRM107 may ultimately be best used soon after surgery to treat this region of tumor-infiltrated brain after resection of all contrast-enhancing volume. In this situation, chloroquine should be greatly restricted from the tumor by the intact BBB. The i.v. injection of chloroquine during intracerebral infusion of Tf-CRM107 may protect the vasculature, permitting less toxicity to the brain while allowing greater doses of Tf-CRM107 to be delivered to tumor to further improve the response rate of this new cancer therapy.

Acknowledgments

We thank Pat Johnson for assistance and Daryl Despres for expertise in MRI manipulation.

References

1. Johnson, V. G., Wilson, D., Greenfield, L., and Youle, R. J. The role of the diphtheria toxin receptor in cytosol translocation. J. Biol Chem., *263:* 1295–1300, 1988.
2. Greenfield, L., Johnson, V. G., and Youle, R. J. Mutations in diphtheria toxin separate binding from entry and amplify immunotoxin selectivity. Science (Washington DC), *238:* 536–539, 1987.
3. Laske, D. W., Ilercil, O., Akbasak, A., Youle, R. J., and Oldfield, E. H. Efficacy of direct intratumoral therapy with targeted protein toxins for solid human gliomas in nude mice. J. Neurosurg., *80:* 520–526, 1994.
4. Laske, D. W., Youle, R. J., and Oldfield, E. H. Tumor regression with regional distribution of the targeted toxin Tf-CRM107 in patients with malignant brain tumors. Nat. Med., *3:* 1362–1368, 1997.

5. Bobo, R. H., Laske, D. W., Akbasak, A., Morrison, P. F., Dedrick, R. L., and Oldfield, E. H. Convection-enhanced delivery of macromolecules in the brain. Proc. Natl. Acad. Sci. USA, *91:* 2076–2080, 1994.
6. Jefferies, W. A., Brandon, M. R., Hunt, S. V., Williams, A. F., Gatter, K. C., and Mason, D. Y. Transferrin receptor on endothelium of brain capillaries. Nature (Lond.), *312:* 162–163, 1984.
7. Kim, K., and Groman, N. B. In vitro inhibition of diphtheria toxin action by ammonium salts and amines. J. Bacteriol., *90:* 1552–1556, 1965.
8. Sandvig, K., and Olsnes, S. Rapid entry of nicked diphtheria toxin into cells at low pH. Characterization of the entry process and effects of low pH on the toxin molecule. J. Biol. Chem., *256:* 9068–9076, 1981.
9. Donovan, J. J., Simon, M. I., Draper, R. K., and Montal, M. Diphtheria toxin forms transmembrane channels in planar lipid bilayers. Proc. Natl. Acad. Sci. USA, *78:* 172–176, 1981.
10. Sandvig, K., and Olsnes, S. Diphtheria toxin entry into cells is facilitated by low pH. J. Cell Biol., *87:* 828–832, 1980.
11. Draper, R. K., and Simon, M. I. The entry of diphtheria toxin into the mammalian cell cytoplasm: evidence for lysosomal involvement. J. Cell Biol., *87:* 849–854, 1980.
12. Leppla, S., Dorland, R. B., and Middlebrook, J. L. Inhibition of diphtheria toxin degradation and cytotoxic action by chloroquine. J. Biol. Chem., *255:* 2247–2250, 1980.
13. Agarwal, S. C., and Pryce, D. M. Experimental diphtheritic paralysis in rats. J. Path. Bact., *78:* 171–177, 1959.
14. Eisenberg, D., Schwarz, E., Komaromy, M., and Wall, R. Analysis of membrane and surface protein sequences with the hydrophobic moment plot. J. Mol. Biol., *179:* 125–142, 1984.
15. Oh, K. J., Zhan, H., Cui, C., Hideg, K., Collier, R. J., and Hubbell, W. L. Organization of diphtheria toxin T domain in bilayers: a site-directed spin labeling study. Science (Washington DC), *273:* 810–812, 1996.
16. Seelig, A., Gottschlich, R., and Devant, R. M. A method to determine the ability of drugs to diffuse through the blood-brain barrier. Proc. Natl. Acad. Sci. USA, *91:* 68–72, 1994.
17. Yamada, K., Ushio, Y., Hayakawa, T., Kato, A., Yamada, N., and Mogami, H. Quantitative autoradiographic measurements of blood-brain barrier permeability in the rat glioma model. J. Neurosurg., *57:* 394–398, 1982.
18. Chamberlain, M. C., Murovic, J. A., and Levin, V. A. Absence of contrast enhancement on CT brain scans of patients with supratentorial malignant gliomas. Neurology, *38:* 1371–1374, 1988.
19. Gustafsson, L. L., Walker, O., Alvan, G., Beermann, B., Estevez, F., Gleisner, L., Lindstrom, B., and Sjoqvist, F. Disposition of chloroquine in man after single intravenous and oral doses. Br. J. Clin. Pharmacol., *15:* 471–479, 1983.
20. Aderounmu, A. F., Salako, L. A., Lindstrom, B., Walker, O., and Ekman, L. Comparison of the pharmacokinetics of chloroquine after single intravenous and intramuscular administration in healthy Africans. Br. J. Clin. Pharmacol., *22:* 559–564, 1986.
21. Scherer, H. J. The forms of growth in gliomas and the practical significance. Brain, *63:* 1–35, 1940.
22. Greene, G. M., Hitchon, P. W., Schelper, R. L., Yuh, W., and Dyste, G. N. Diagnostic yield in CT-guided stereotactic biopsy of gliomas. J. Neurosurg., *71:* 494–497, 1989.
23. Kelly, P. J., Daumas-Duport, C., Kispert, D. B., Kall, B. A., Scheithauer, B. W., and Illig, J. J. Imaging-based stereotaxic serial biopsies in untreated intracranial glial neoplasms. J. Neurosurg., *66:* 865–874, 1987.